



ELSEVIER

Applied Catalysis B: Environmental 28 (2000) 29–41



www.elsevier.com/locate/apcatb

## Study of the lean NO<sub>x</sub> reduction with C<sub>3</sub>H<sub>6</sub> in the presence of water over silver/alumina catalysts prepared from inverse microemulsions

A. Martínez-Arias<sup>a,\*</sup>, M. Fernández-García<sup>a</sup>, A. Iglesias-Juez<sup>a</sup>, J.A. Anderson<sup>b</sup>,  
J.C. Conesa<sup>a</sup>, J. Soria<sup>a</sup>

<sup>a</sup> Instituto de Catálisis y Petroleoquímica, CSIC, Campus UAM, Camino de Valdelatas, s/n. Cantoblanco, 28049 Madrid, Spain

<sup>b</sup> Chemistry Department, University of Dundee, Dundee DD1 4HN, Scotland, UK

Received 20 February 2000; received in revised form 8 April 2000; accepted 8 April 2000

### Abstract

A study of the lean NO<sub>x</sub> reduction activity with propene in the presence of water over Ag/Al<sub>2</sub>O<sub>3</sub> catalysts with different silver loadings (1.5–6 wt. %), prepared by precipitation from inverse microemulsions, has been performed. The highest NO<sub>x</sub> reduction activities were observed for catalysts with intermediate silver loadings. Complementary in situ-DRIFTS results on one of the active catalysts indicate formation of surface adsorbed acrylate and nitrate species resulting from oxidation of propene and NO, and of isocyanate and cyanide species, which are final intermediates in the NO<sub>x</sub> reduction process. Comparison by in situ-DRIFTS between one of the active catalysts (with 1.5 wt. % Ag) and an inactive one (with 6 wt. % Ag) reveals that a certain nitrate concentration is maintained under reaction conditions at the surface of active catalysts. This is attributed to the existence of different NO<sub>x</sub> reaction paths, involving interaction of activated NO<sub>x</sub> species with acidic hydroxyls of the alumina surface for active catalysts. Characterisation results by XRD and TEM indicate that amorphous silver-containing phases which are active for NO<sub>x</sub> reduction lie over a wide range of particle sizes, while the different size of these entities before and after reaction indicates significant mobility under reaction conditions. © 2000 Elsevier Science B.V. All rights reserved.

**Keywords:** NO<sub>x</sub>-propene SCR; Ag/Al<sub>2</sub>O<sub>3</sub> catalysts; In situ-DRIFTS; XRD; TEM

### 1. Introduction

Selective catalytic reduction (SCR) of NO<sub>x</sub> in the oxygen rich exhaust streams of lean burn engines remains one of the major challenges for environmental catalysis. Cu-ZSM-5 was the first catalyst displaying good lean NO<sub>x</sub> reduction activity, after the discovery by Iwamoto et al. [1] that this system is particularly active for NO decomposition in the presence of O<sub>2</sub>. However, it was later shown that this catalyst lacks the

stability required for operation in high temperature exhausts containing water and/or SO<sub>2</sub> [2,3], a problem which can be generally extended to all zeolite-based systems [4]. Best results in this respect have been observed when using alumina supported systems [5,6]. Among them, Pt and Pd catalysts have shown high activity for the reaction, presenting NO<sub>x</sub> conversion windows at much lower temperatures than zeolite based catalysts [7]. They are, however, highly selective towards N<sub>2</sub>O, an undesirable greenhouse gas [8].

Alumina supported silver is an effective catalyst for lean NO reduction with C<sub>3</sub>H<sub>6</sub> [6,9]. The catalytic activity of this material is maintained at a relatively high

\* Corresponding author. Fax: +34-91-5854760.

E-mail address: amartinez@icp.csic.es (A. Martínez-Arias)

level even in the presence of  $\text{H}_2\text{O}$  and  $\text{SO}_2$  [9,10]. Higher NO conversions, and at lower temperatures, are generally observed when using oxygenated hydrocarbons, such as ethanol and acetone as reductants instead of propene [9]. Unfortunately, harmful by-products, such as hydrogen cyanide, can be formed when using those oxygenated reductants [11].

The effectiveness of the  $\text{Ag}/\text{Al}_2\text{O}_3$  catalyst depends greatly on the Ag loading, best catalytic performance being achieved with intermediate loadings (2–3%) [9,12]. Higher silver loadings produce higher rates of  $\text{C}_3\text{H}_6$  oxidation with  $\text{O}_2$ , at the expense of its reaction with NO. This has been attributed to the detrimental effect of increasing the particle size of silver oxide entities, yielding reducible entities (leading to  $\text{Ag}^0$ ) more readily with a higher activity for non-selective propene oxidation [12]. It has been proposed that for lower size clusters, silver can be stabilised in an oxidised ( $\text{Ag}^+$ ) state, as a consequence of the interaction with the alumina support, which would constitute the active centres for the  $\text{NO}_x$  reduction reaction [12]. In this respect, an  $\text{Ag}/\text{Al}_2\text{O}_3$  catalyst has been reported to improve markedly in performance after an XRD-detectable silver aluminate phase is generated by hydrothermal treatment at 1073 K [13]. It may also be recalled that, when present as cations exchanged in zeolites, i.e. a situation where it is less easy to form large particles of oxide or metal,  $\text{NO}_x$  conversion (using  $\text{CH}_4$  as reductant) does not decrease with Ag loading increasing up to ca. 10% by weight [14].

The aim of the present work is to study the catalytic activity in lean NO reduction with  $\text{C}_3\text{H}_6$  in the presence of water for  $\text{Ag}/\text{Al}_2\text{O}_3$  catalysts prepared by precipitating silver entities from inverse microemulsions, a preparation method which is most appropriate in obtaining nanosized particles [15].

## 2. Experimental

Alumina supported silver catalysts of different Ag loadings were prepared using  $\text{AgNO}_3$  (supplied by Aldrich) as silver precursor and  $\text{Al}_2\text{O}_3$  (Condea,  $S_{\text{BET}}=200\text{ m}^2\text{ g}^{-1}$ ) as support. Aqueous solutions containing different  $\text{AgNO}_3$  concentrations (in order to obtain final nominal silver loadings of 1.5, 3 and 6 wt.%) were prepared. For each of these solutions, an inverse microemulsion (water in organic) was

prepared by mixing while stirring 50 g of the aqueous solution with 427 g of heptane, 92 g of hexanol and 89 g of a surfactant (Triton X-100, supplied by Aldrich). Then, the appropriate amount of alumina was introduced to the microemulsion, stirring the resulting suspension during 1 h prior to mixing with a microemulsion of similar characteristics, containing an aqueous solution of tetramethylammonium hydroxide pentahydrate (Aldrich) in concentrations similar to those of the corresponding  $\text{AgNO}_3$  solutions, used as precipitating agent. The mixture was then stirred for 24 h, after which the resulting suspension was centrifuged and decanted, the remaining solid being washed with methanol, centrifuged and decanted again. The solid was then dried for a short period at room temperature, then at 383 K for 24 h, and finally calcined in air at 773 K for 2 h. Ag analyses of the samples by ICP-AES yielded values which coincide, within the error limits, with the nominal values, which indicate that a thorough silver precipitation was achieved in all cases. Samples are denoted as 1.5Ag, 3Ag and 6Ag, in accordance with the weight loadings. The BET surface areas showed values similar to that of the parent alumina. A portion of the 3Ag catalyst calcined at 773 K was further calcined in air at 1073 K for 2 h.

Powder XRD patterns were recorded on a Siemens D-500 diffractometer using nickel-filtered  $\text{Cu K}\alpha$  radiation operating at 40 kV and 25 mA and with a  $0.025^\circ$  step size.

Samples for transmission electron microscopy (TEM) were prepared by crushing in an agate mortar, dispersing in isobutanol, and depositing on perforated carbon films supported on copper grids. The TEM data were obtained on a JEOL 2000 FX II system (with 3.1 point resolution) equipped with a LINK probe for energy-dispersive analysis (EDX).

Catalytic activity tests were performed in a pyrex flow reactor system using a feed stream consisting of 0.1% NO, 0.1%  $\text{C}_3\text{H}_6$ , 5%  $\text{O}_2$  and 3%  $\text{H}_2\text{O}$  ( $\text{N}_2$  balance; ca.  $1 \times 10^3\text{ cm}^3\text{ min}^{-1}\text{ g}^{-1}$  at a fixed space velocity of  $4 \times 10^4\text{ h}^{-1}$ ). The effluent from the reactor, with the exception of  $\text{H}_2\text{O}$  which was (mostly) removed by a cold trap ( $\text{NaCl}$ -ice mixture), was analysed on line using a Perkin-Elmer 1725X FTIR spectrometer coupled with a multiple reflection transmission cell (Infrared Analysis Inc.). In all cases, the samples were subjected to a calcination pretreatment in situ in dry air

at 773 K. Typical tests were performed in the light-off mode by increasing the temperature of the feed stream from 298 to 823 K at  $5\text{ K min}^{-1}$ .

In situ-DRIFTS experiments were performed using a Perkin-Elmer 1750 FTIR fitted with an MCT detector. The DRIFTS cell (Harrick) was equipped with  $\text{CaF}_2$  windows and a heating cartridge that allowed samples to be heated up to 773 K. The spectral resolution employed was  $4\text{ cm}^{-1}$ . Samples of ca. 80 mg were calcined in situ in dry air at 773 K. The spectra were taken by accumulating 25 scans, except where noted otherwise. The composition of the inlet gases was manipulated by a computer controlled gas blender with  $80\text{ cm}^3\text{ min}^{-1}$  passing through the catalyst bed, and with the  $\text{NO}_x$  gases in the outlet from the DRIFTS cell monitored by a chemiluminescence analyser (Thermo Environmental Instruments 42C high level analyser).

### 3. Results

#### 3.1. Catalytic activity tests

Fig. 1 shows the propene and  $\text{NO}_x$  ( $\text{NO} + \text{NO}_2$ ) conversions, along with the yields of  $\text{NO}_2$  and CO for the  $\text{C}_3\text{H}_6$ -SCR of NO in the presence of water. No other nitrogen or carbon containing product except  $\text{CO}_2$  (e.g.  $\text{N}_2\text{O}$  or oxygenated hydrocarbons) was detected in the evolved gases, indicating that  $\text{NO}_x$  is fully converted to  $\text{N}_2$  and that no products resulting from partial oxidation of propene (with the exception of CO) were formed. The absence of  $\text{N}_2\text{O}$  and the detection of CO contrast with previous studies in which a certain (generally small and dependent on silver loading)  $\text{N}_2\text{O}$  selectivity and full propene combustion was observed for  $\text{Ag}/\text{Al}_2\text{O}_3$  catalysts [12,16]. The alumina support showed very low SCR activity, which can be attributed to the deactivation of the system induced by the presence of water [12].

The results indicate the promoting effect of silver at intermediate loadings on the SCR reaction, in agreement with a previous report [9]. The results observed for sample 6Ag show certain similarities with previous reports [8,12], in the sense that low  $\text{NO}_x$  conversion levels are achieved over alumina supported samples with relatively high silver loadings, while relatively higher non-selective  $\text{C}_3\text{H}_6$  combustion is achieved. On

the other hand, 1.5Ag and 3Ag are active for  $\text{NO}_x$  reduction, showing similar  $\text{NO}_x$  and  $\text{C}_3\text{H}_6$  conversion profiles. A certain correlation is found between the  $\text{NO}_x$  reduction activity and the presence of higher amounts of  $\text{NO}_2$  at temperatures at which  $\text{NO}_x$  reduction activity starts for the 1.5Ag and 3Ag samples. Comparison of the  $\text{NO}_x$  reduction activity of these two samples reveals only subtle differences for  $T < \text{ca. } 673\text{ K}$  at which low  $\text{NO}_x$  conversions are observed, which, in view of the absence of  $\text{C}_3\text{H}_6$  oxidation under these conditions and the absence of other N-containing products, can be attributed to  $\text{NO}_x$  adsorption phenomena.

In previous studies, the SCR catalytic activity of alumina-promoted catalysts had been improved by subjecting them to high calcination temperatures (typically 1073 K [13,16]), which has been attributed to formation of aluminate phases which are less efficient for the non-selective combustion of the reductant than the corresponding alumina-supported oxides [13,16]. A similar pretreatment was performed here for the 3Ag catalyst. As shown in Fig. 1, this pretreatment produces a slight lowering of the  $\text{NO}_x$  reduction activity of the system while maintaining roughly similar profiles as the parent 3Ag catalyst for  $\text{C}_3\text{H}_6$  conversion, and  $\text{NO}_2$  and CO yields.

#### 3.2. In situ-DRIFTS experiments

DRIFT spectra of the fresh 1.5Ag and 6Ag samples calcined in dry air, recorded at 298 K, are shown in Fig. 2. Both samples display bands in the hydroxyl stretching region of a similar nature at 3731 (with a higher frequency shoulder), 3680 and  $3620\text{ cm}^{-1}$ , and a broader one below  $3600\text{ cm}^{-1}$  showing a maximum at  $3573\text{ cm}^{-1}$  and a shoulder at lower frequency extending to ca.  $3500\text{ cm}^{-1}$ . A slightly greater intensity at  $3573\text{--}3550\text{ cm}^{-1}$  for 1.5Ag was the only significant difference between the samples. These bands can all be attributed to diverse surface Al–OH groups. Bands in the  $3800\text{--}3600\text{ cm}^{-1}$  region correspond to different isolated hydroxyl species, their frequency being related to the nature of the Al cation and/or to the coordination number of the corresponding hydroxyl group [17,34]. On the other hand, features at  $3573\text{--}3500\text{ cm}^{-1}$  can be assigned to associated (mutually interacting by hydrogen bonds) hydroxyl groups [17,34]. The spectra of both samples also show bands

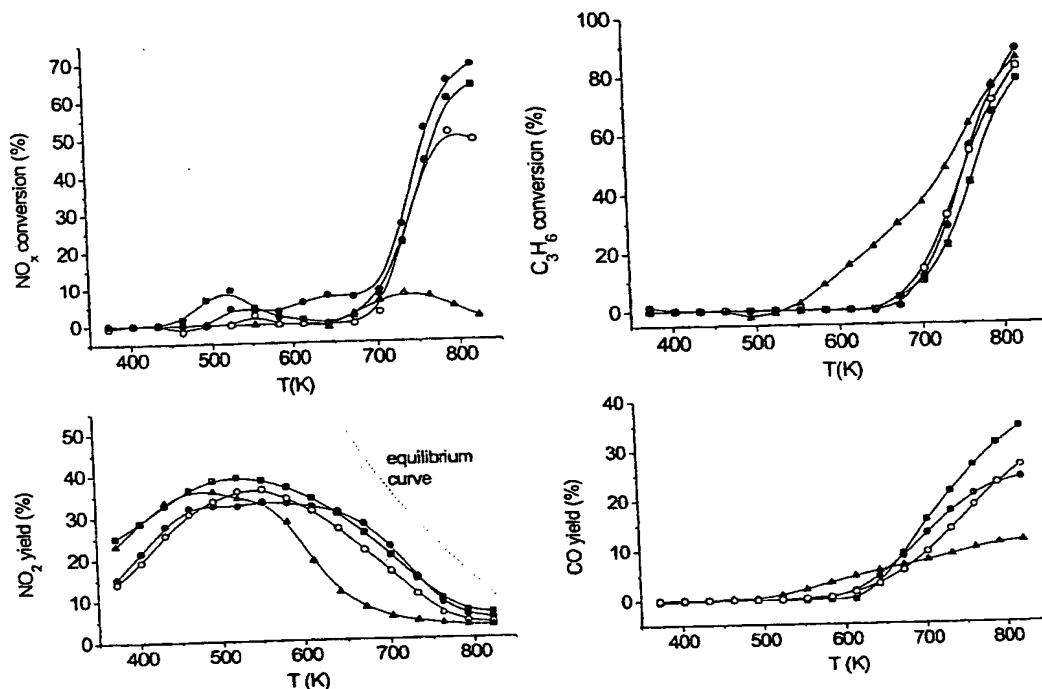


Fig. 1. Catalytic activity results for  $C_3H_6$ -SCR of NO over the  $Ag/Al_2O_3$  catalysts. Squares: 1.5Ag; full circles: 3Ag; open circles: 3Ag calcined at 1073 K; triangles: 6Ag. The dotted line in the bottom left plot represents the thermodynamic limit associated to the reaction  $NO + 1/2O_2 \leftrightarrow NO_2$ .

at 1655, 1438 and 1228 attributed to residual alumina hydrogencarbonate species [18]. Other features at 1554–1520, 1353–1340 and 1252  $cm^{-1}$  were apparent in sample 6Ag, although they may also be present with a lower intensity in sample 1.5Ag. These suggest different  $CO_x$  (carbonates or carboxylate species) and/or  $NO_x$  (nitrates or nitrites) species [19]. The greater intensity at higher silver loading suggests that these bands may originate from incomplete decomposition of precursors employed for silver deposition during the preparation procedure.

DRIFT spectra of sample 1.5Ag recorded under reaction conditions are shown in Fig. 3. The results show that hydrogen carbonate species present in the initial sample (Fig. 3a) are not involved in the reaction as they have already disappeared at  $T \leq 573$  K. These spectra show the generation of species giving a band at 1546  $cm^{-1}$  and a shoulder at ca. 1250  $cm^{-1}$ ,

which are present at  $T \geq 573$  K, and bands or shoulders at 1576, 1457, 1377 and 1294  $cm^{-1}$  appearing for  $T \geq 673$  K. Both groups of bands show increasing intensity with reaction temperature. Additionally, certain modifications to the hydroxyl species are produced during the course of reaction, the most intense of which appear at 3716, 3677 and 3567  $cm^{-1}$  in the spectrum recorded at 773 K (Fig. 3d). Careful inspection of the 2400–2000  $cm^{-1}$  region (inset of Fig. 3), reveals the formation of gas phase  $CO_2$  giving bands at 2372 and 2345  $cm^{-1}$ , in good agreement with the activity data (Fig. 1), and of weak bands at 2243 and 2167  $cm^{-1}$ , due to chemisorbed isocyanate and cyanide species, respectively [20], for the experiment performed at 773 K. These latter species have been proposed as final intermediates in the  $NO_x$  reduction process: isocyanate species readily decompose to the final products upon interaction with NO and/or

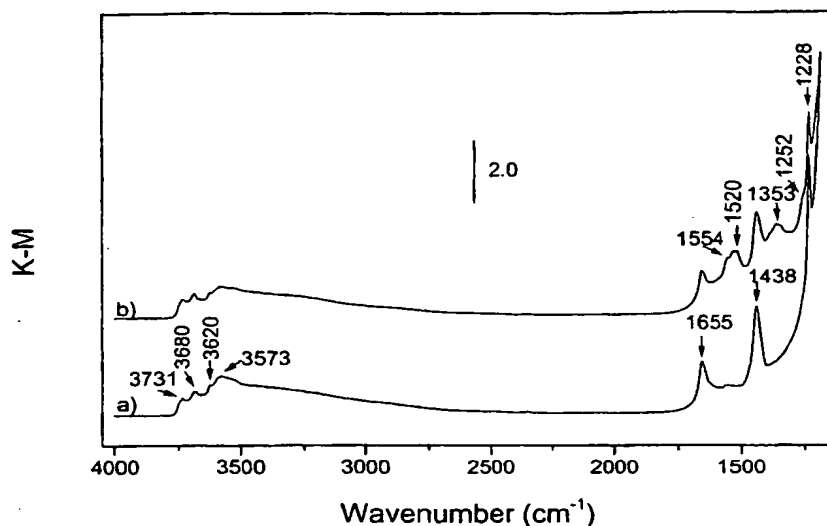


Fig. 2. DRIFTS spectra of the initial calcined samples (a) 1.5Ag; (b) 6Ag.

O<sub>2</sub> [20–22], while cyanide species, although showing lesser activity [16,22], are also thought to be involved in the process either directly interacting with the reactant mixture [22] or through their conversion

to isocyanate species [23]. Their detection in spectra recorded at 773 K is consistent with the observation of NO<sub>x</sub> reduction activity at this temperature for this catalyst.

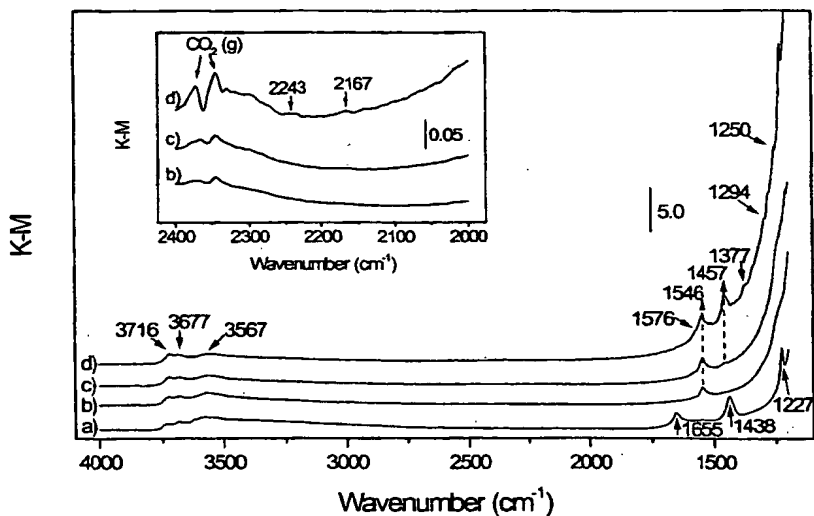


Fig. 3. In situ-DRIFTS spectra of 1.5Ag. (a) Initial calcined sample recorded at room temperature. Spectra recorded under reaction conditions: 0.1% NO, 0.1% C<sub>3</sub>H<sub>6</sub>, 5% O<sub>2</sub> and 3% H<sub>2</sub>O (N<sub>2</sub> balance, total flow=100 cm<sup>3</sup> min<sup>-1</sup>); at (b) 573, (c) 673 and (d) 773 K.

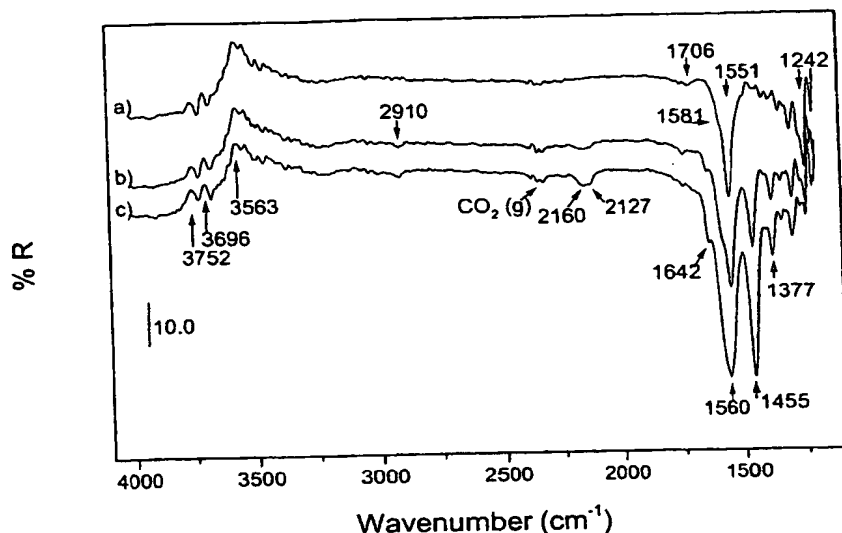


Fig. 4. In situ-DRIFTS spectra of 1.5Ag recorded at 723 K in (a) 0.16% NO+5% O<sub>2</sub>. Subsequent addition of (b) 0.08% C<sub>3</sub>H<sub>6</sub> and (c) 0.16% C<sub>3</sub>H<sub>6</sub> to the reactant flow.

In order to identify the different species observed in the infrared spectra and to obtain further insight into the catalytic behaviour of these systems, infrared spectra were obtained for samples 1.5Ag and 6Ag (Figs. 4 and 5) under reaction conditions using various gas mixtures. To achieve more precise detection of the changes occurring at the catalyst surface upon interaction with the different gases, following the calcination pretreatment in dry air at 773 K under similar conditions as employed for the catalytic tests, the samples were cooled in dry air at 723 K, before switching to inert gas (N<sub>2</sub>) for 15 min and recording the background spectrum under these conditions. The desired reactant gases (diluted in N<sub>2</sub>) were then flown through the cell at that temperature (leaving at least 10 min contact with the corresponding reactant gases in every case) and the changes occurring in the infrared spectra were recorded (100 scans being accumulated for these experiments). At this recording temperature (723 K), significant NO<sub>x</sub> reduction activity was observed for sample 1.5Ag while sample 6Ag was almost inactive (Fig. 1).

Introduction of NO+O<sub>2</sub> produces two main bands in the spectra of both samples (Figs. 4 and 5a) at ca. 1550 (with a higher frequency shoulder) and ca.

1245 cm<sup>-1</sup>, that can be attributed to different (monodentate and bidentate) nitrate species adsorbed on the alumina surface [24,25]. A small band at 1706 cm<sup>-1</sup> was also noted in the case of sample 1.5Ag (Fig. 4a). The small differences in the frequencies of bands due to nitrate species between both samples can be ascribed to slight differences in the local environment of adsorption sites of the nitrate species. This is shown in the OH stretching region of the spectra where negative bands are concomitantly produced for sample 1.5Ag, particularly affecting the more acidic hydroxyls at 3563 cm<sup>-1</sup>, and to a lesser extent the less acidic hydroxyls at 3696 and 3752 cm<sup>-1</sup>. This indicates that the NO<sub>x</sub> adsorption process involves, at least to some extent, interactions with specific hydroxyl species of this sample, whereas no such pronounced changes occur in the hydroxyl species of sample 6Ag.

Subsequent addition of C<sub>3</sub>H<sub>6</sub> to the flowing gas mixture (Figs. 4b–c and 5b–c) produced the appearance of a group of bands at 1642, 1572–1560, 1455, 1377 and 1298 cm<sup>-1</sup> (along with a weaker band at 2910 cm<sup>-1</sup>) for both samples. Also, certain changes were noted in the hydroxyl stretching region upon introduction of propene, involving mainly a decrease in intensity at 3752 cm<sup>-1</sup>, which was more significant for

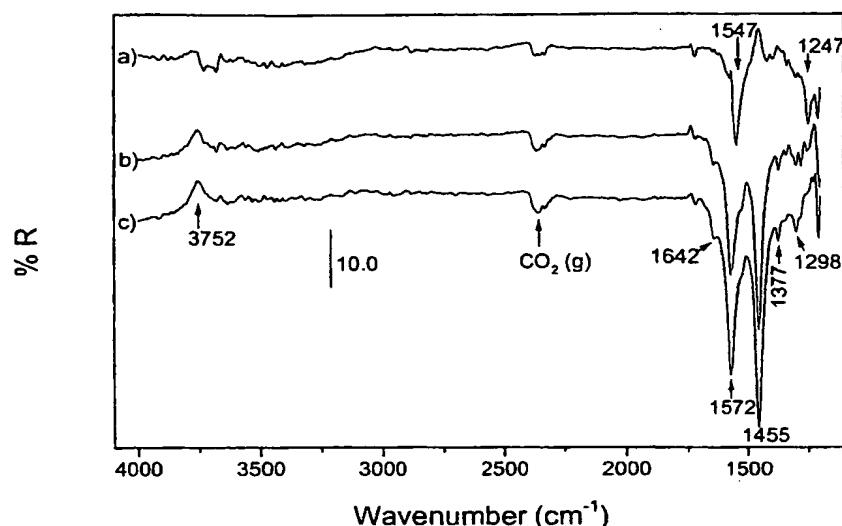


Fig. 5. In situ-DRIFTS spectra of 6Ag recorded at 723 K in (a) 0.16% NO+5% O<sub>2</sub>. Subsequent addition of (b) 0.08% C<sub>3</sub>H<sub>6</sub> and (c) 0.16% C<sub>3</sub>H<sub>6</sub> to the reactant flow.

sample 6Ag. A slight recovery of the acidic hydroxyl band at  $3563\text{ cm}^{-1}$  was observed for 1.5Ag; this effect being more pronounced when NO was eliminated from the gas mixture. Other differences between the samples include the exclusive appearance of bands at 2160 and  $2127\text{ cm}^{-1}$  for sample 1.5Ag, which disappeared when NO was removed from the gas flow. Both bands can be attributed to cyanide species adsorbed at different sites of the catalyst [21,22]. Additionally, differences in the evolution of nitrate bands for both samples were produced upon C<sub>3</sub>H<sub>6</sub> incorporation. Nitrate species were diminished for sample 6Ag upon introduction of 800 ppm C<sub>3</sub>H<sub>6</sub> to the reactant flow and were strongly depleted in the presence of 1600 ppm C<sub>3</sub>H<sub>6</sub> (only a small shoulder at ca.  $1530\text{ cm}^{-1}$  was detected, which might correspond to such nitrate species [25]). In contrast, although a certain depletion of nitrate species was produced for sample 1.5Ag upon introduction of C<sub>3</sub>H<sub>6</sub>, these species were still present in detectable quantities even after introduction of 1600 ppm, under conditions which approximate those employed for the catalytic tests in which equimolar amounts of NO and C<sub>3</sub>H<sub>6</sub> were employed. This analysis was mainly based on the evolution shown by the non-overlapping nitrate band

at ca.  $1245\text{ cm}^{-1}$ . A good correlation could also be noted between the loss of intensity of this band and a greater blue shift of the band at  $1572\text{--}1560\text{ cm}^{-1}$ , which showed reduced width and a lower relative intensity with respect to the band at  $1455\text{ cm}^{-1}$ . These facts suggest that the feature at  $1572\text{--}1560\text{ cm}^{-1}$  for 1.5 Ag (Fig. 4c) could be formed by overlap between a band due to nitrate (at lower wavenumbers) and an adsorbed C<sub>3</sub>H<sub>6</sub>-derived species giving a band at higher wavenumbers in that region, as will be analysed below. On the other hand, subsequent introduction of 3% H<sub>2</sub>O did not produce any significant changes in the spectra of either of the samples, except for a slight recovery of intensity of the hydroxyl at  $3563\text{ cm}^{-1}$  for sample 1.5Ag.

As uncertainty exists in respect to assignment of the bands at 1642 and  $1377\text{ cm}^{-1}$  to N-containing organic compounds (organo-nitrite or oxime species) [16], an experiment was performed by firstly introducing C<sub>3</sub>H<sub>6</sub> and then O<sub>2</sub> to the 1.5Ag sample (Fig. 6a). No changes were apparent in the infrared spectrum after flowing C<sub>3</sub>H<sub>6</sub> (1600 ppm) alone at 723 K, despite considerable darkening of the sample, most likely due to generation of carbonaceous deposits and/or to an extensive sample reduction. Subsequent introduc-

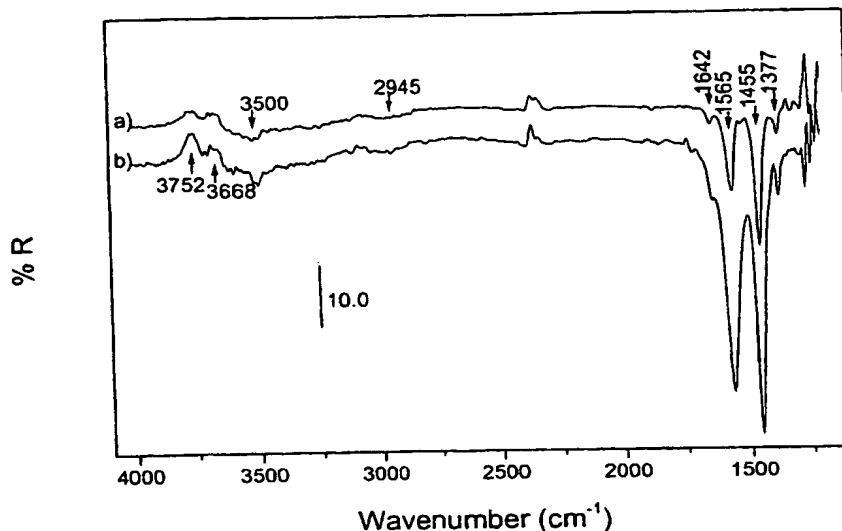


Fig. 6. In situ-DRIFTS spectra of 1.5Ag recorded at 723 K in (a) 0.16%  $C_3H_6$ +5%  $O_2$ . (b) Subsequent incorporation of 0.16% NO to the reactant flow.

tion of 5%  $O_2$  restored the initial white colour to the sample, and generated species giving bands at 1642, 1565, 1455 and 1377  $cm^{-1}$  (and probably also at 1298  $cm^{-1}$ ). This confirms the assignment of these bands to a N-free species. Additionally, a small band at 2945  $cm^{-1}$  was detected (due to C–H stretching vibrations of the corresponding  $C_xH_yO_z$  species) while negative bands due to depletion of hydroxyls at 3752 and 3668  $cm^{-1}$  were observed and a hydroxyl at ca. 3500  $cm^{-1}$  was generated. Interestingly, no  $NO_x$  reduction was detected in this case, in correlation with the failure to detect cyanide or isocyanate bands, upon subsequent NO incorporation to the gas mixture, indicating that the sample was deactivated by the initial contact with propene. No indication to suggest reactivity of the more acidic hydroxyl species was observed under these conditions (Fig. 6b). The spectrum shown in Fig. 6a shows certain similarities with that observed for propionic acid adsorption on  $\gamma-Al_2O_3$  [24], suggesting that the corresponding adsorbed species are propionate complexes. Analysis of the spectrum suggests, however, that a C=C double bond is present in the adsorbed complex. The most intense bands at 1565 and 1455  $cm^{-1}$  indicate the  $\nu_{as}COO$  and  $\nu_{s}COO$  stretching modes, respectively, of a carboxylate group. The

band at 1642  $cm^{-1}$  is characteristic of the existence of unsaturated bonds being attributed to the  $\nu_{C=C}$  stretching mode, while the band at 1377  $cm^{-1}$  can be attributed to the  $\delta_{C-H}$  vibration [19,26]. It is important to note that  $\nu_{C-C}$  vibrations would be expected to appear at wave numbers below ca. 1300  $cm^{-1}$ ; thus, the presence of a band at 1640  $cm^{-1}$  is not expected for a saturated organic-carboxylate complex [19]. In this sense, the band which eventually appears simultaneously in some of the spectra at 1298  $cm^{-1}$  (Figs. 4 and 5) can be assigned to the  $\nu_{C-C}$  vibration. Most likely assignment for such a species would be to an unsaturated organic-carboxylate compound such as an adsorbed acrylate species. Observation of similar bands following acrolein adsorption on  $Rh/Al_2O_3$ , was attributed to surface acrylate species formed by oxidation of acrolein [26]. Similar species were generated by reaction of propene and NO over the same catalyst [26].

### 3.3. XRD and TEM results

The XRD patterns of the 3Ag and 6Ag samples in their initial calcined states and after reaction up to 823 K are shown in Fig. 7. Both samples inde-



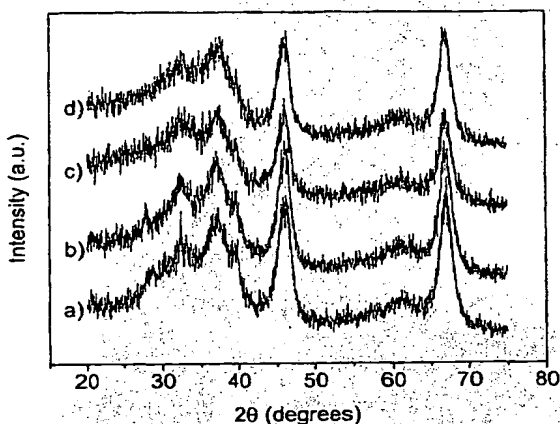


Fig. 7. The XRD of (a) initial 3Ag; (b) post-reaction 3Ag; (c) initial 6Ag; (d) post-reaction 6Ag.

pendent of pretreatment history showed very similar patterns dominated by the  $\gamma$ - $\text{Al}_2\text{O}_3$  component. No peaks attributable to Ag,  $\text{Ag}_2\text{O}$  or AgO phases were detected. The absence of diffracting properties for the Ag-containing phases was confirmed by the use of electron diffraction (data not shown).

Analysis of the TEM images gave evidence of the significant size reached by the Ag-containing particles after reaction (following the tests shown in Fig. 1); the average size being 10 nm for the 1.5Ag specimen and 24 nm in the case of 3Ag. As an example, Fig. 8A contains a micrograph taken for the latter sample. Apart from the average particle size, this figure illustrates the broad particle size distribution present after reaction. Fig. 8B also contains a micrograph of the 3Ag catalyst before reaction which shows a smaller average particle size of ca. 12 nm as well as a significantly narrow particle size distribution. The behaviour observed for this sample under reaction, i.e. significant aggregation of the Ag-containing particles and broadening of the corresponding distribution, was symptomatic of all catalysts studied. On the other hand, correlation of this data with those of diffraction techniques permits the conclusion that the formation of amorphous phases only occurs during the preparation procedure, and that these are stable under reaction conditions, in respect to the lack of long-range order.

#### 4. Discussion

Several research groups have investigated the reaction mechanism of NO-SCR with hydrocarbons [16,22,24]. Although no general agreement can be found in the proposed mechanisms, it is generally agreed that for catalysts showing low  $\text{N}_2\text{O}$  selectivity, either the hydrocarbon or the NO (or both) have to be previously activated by formation of some oxidised intermediates (in general terms,  $\text{C}_x\text{H}_y\text{O}_z$  for the hydrocarbon and  $\text{NO}_2$  or surface  $\text{NO}_2$  for the NO). These then interact with  $\text{NO}_x$  or the hydrocarbon (preactivated or not) to yield nitrogen-containing organic intermediates ( $\text{R-NO}_x$ ). These decompose possibly via more simple adsorbed isocyanate or cyanide groups which finally yield the reaction products upon interaction with NO and/or  $\text{O}_2$  [20–22]. Consistent with this, in the case of neat alumina, it has been shown that both adsorbed acetate or nitrate species (generated under NO-propene lean conditions) can react with  $\text{NO} + \text{O}_2$  or  $\text{C}_3\text{H}_6$ , respectively, to yield the final products [24]. The promoting effect of silver incorporation to the alumina catalysts has been demonstrated by different groups [6,9,12,16], although the role of each of the catalyst components is still uncertain. In a recent study, it was proposed that the role of silver at relatively low loadings (giving the most active catalysts) was related to the increased rates of formation of  $\text{R-NO}_x$  compounds, in agreement with the higher rates of formation of adsorbed nitrate species (from which the former are proposed to be created), which predominate under reaction conditions [16]. Consistent with this, the results obtained by in situ-DRIFTS for sample 1.5Ag (Figs. 3 and 4) show that detectable quantities of nitrate species were present when  $\text{NO}_x$  reduction activity is produced. This contrasts with the behaviour of sample 6Ag for which a significantly lower amount of nitrate species is present under reaction conditions, being strongly depleted upon introduction of propene in the reaction mixture (Fig. 5). Such rapid consumption of adsorbed nitrate species for 6Ag could be related with the generation of partial oxidation products of propene which are particularly reactive towards adsorbed nitrate species. This interaction would then lead to particular  $\text{R-NO}_x$  compounds which would decompose back to  $\text{NO}_x$  instead of yielding  $\text{NO}_x$  reduction products. However, this hypothesis does not seem very proba-

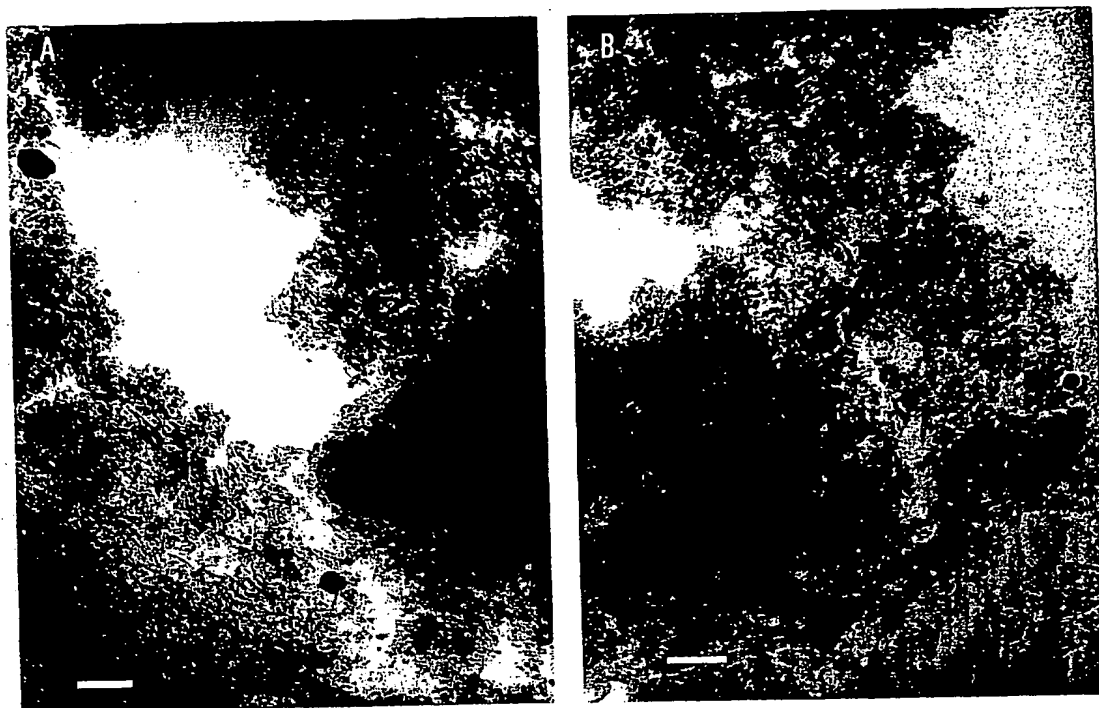
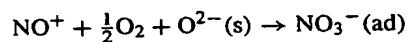


Fig. 8. Bright-field TEM pictures of (A) post-reaction 3Ag and (B) initial 3Ag. The horizontal scales correspond to 50 nm.

ble given that no indication of the presence of such intermediates was obtained in the infrared spectra and that certain lower  $\text{NO}_2$  yield is observed for that catalyst at 700–800 K. The differences observed in the infrared spectra between both samples suggest an important role of hydroxyl species present in sample 1.5Ag. The more acidic associated hydroxyls at the alumina surface (Fig. 4), are involved in the  $\text{NO}_x$  activation processes of that sample. This opens up a new pathway for  $\text{NO}_x$  activation that could produce a more facile regeneration of surface nitrate species leading to observation of a certain amount of these species under reaction conditions. The role of acidic hydroxyls in this reaction has been studied in certain detail in the case of acidic mordenites or H-ZSM-5 catalysts [27,28]. In those cases,  $\text{NO}_x$  activation by interaction with acidic hydroxyls was thought to proceed by generation of nitrosonium ions ( $\text{NO}^+$ ) in a process involving  $\text{H}^+$  (proceeding from the corresponding hydroxyls) consumption [27,28]. In the case

of alumina-promoted catalysts, for which such species have not been detected, the nitrosonium ions could rapidly react with surface oxide ions and with oxygen to yield, either directly or through adsorbed nitrite intermediates, the observed adsorbed nitrate species:



As observed in the infrared spectra (Fig. 4), the corresponding acidic hydroxyls are recovered by interaction with propene (or with intermediate products resulting from partial oxidation of this) thus closing the adsorbed nitrate production cycle.

Production of significant amounts of carbon monoxide appears to be a characteristic of acidic catalysts, as shown by Gerlach et al. [29] for acidic mordenites. In that case, the ratio  $\text{CO}:\text{CO}_2$  produced in the  $\text{NO}_2\text{--C}_3\text{H}_6$  reaction in excess oxygen approached a 1:2 value, which is close to that observed for the active catalysts (1.5Ag and 3Ag) used here. According to previous studies [29], this suggests that the mecha-

nism could involve either R-NO<sub>x</sub> intermediates of the acrylonitrile-type or proceed by oxidation of acrylic acid (or adsorbed acrylate) by NO<sub>2</sub> or nitrate species. In fact, observation of adsorbed acrylate [26] as a product of partial oxidation of propene (Figs. 3–5) correlates well with these proposals. It should be noted that such R-NO<sub>x</sub> intermediates have not been detected in any case, which could be due to their short lifetimes at the temperatures at which the catalysts are active for NO<sub>x</sub> reduction [30,31].

According to the TEM results, the size of the silver entities active for NO<sub>x</sub> reduction (those present in 1.5Ag and 3Ag catalysts) could vary in a relatively wide range (10–24 nm). It should be noted that these variations could lead to small differences in the reaction mechanisms operating in each case, in agreement with the slight differences observed in the reactivity profiles of these samples (Fig. 1). Another interesting point extracted from the TEM results concern the significant changes of the particle size of silver entities observed in the comparison of TEM pictures before and after reaction (Fig. 8). This suggests that the silver entities active for the reaction present a significant mobility which contrasts with proposals suggesting that these entities are strongly stabilized by interaction with the alumina support [12] or by formation of silver aluminate microphases [13]. Further experiments are required to clarify these aspects.

Analysis of NO<sub>x</sub> and C<sub>3</sub>H<sub>6</sub> conversion obtained for 6Ag suggests that the low NO<sub>x</sub> conversion level achieved can be partially attributed to a lack of hydrocarbon resulting from the higher non-selective propene combustion activity of this catalyst. This is in agreement with previous results for Ag/Al<sub>2</sub>O<sub>3</sub> samples with relatively high silver loadings [12,16]. This larger propene combustion capability could also explain the lower CO yield observed for this sample. However, analysis of the NO<sub>x</sub> and C<sub>3</sub>H<sub>6</sub> conversion profiles (particularly in the 700–800 K range) of this catalyst in comparison with samples 1.5Ag and 3Ag, along with the assumption that a linear response of the NO<sub>x</sub> reduction activity with propene concentration is achieved [5,16,32], indicate that the relatively low NO<sub>x</sub> conversion achieved by this system is not only due to a hydrocarbon shortage but also to an intrinsically lower NO<sub>x</sub> reduction activity. This can be related with the lack of formation of a sufficient amount of adsorbed nitrate species under reaction conditions, as

mentioned above. In this context, some differences are observed between the catalytic behaviour of sample 6Ag and that shown by high silver loaded Ag/Al<sub>2</sub>O<sub>3</sub> samples in other reports [12,16]. In the latter cases, a significantly higher C<sub>3</sub>H<sub>6</sub> combustion activity was observed while NO<sub>x</sub> reduction produced substantial amounts of N<sub>2</sub>O. It has been proposed [16] that a different NO reduction mechanism exists involving NO (and O<sub>2</sub>) dissociation and further recombination to N<sub>2</sub>O and N<sub>2</sub> over metallic silver particles present as a consequence of the lower silver dispersion (and thus of the lesser silver/alumina interaction which fails to stabilise active, oxidised silver states [12]). This parallels the mechanism proposed in the case of supported Pt catalysts [8]. The greater non-selective propene combustion capability has been related to the greater activation of both oxygen and propene which may occur in the presence of metallic silver [12,16]. In our case, it is not clear whether the lower NO<sub>x</sub> reduction activity of 6Ag is the result of generation of metallic silver under reaction conditions since such a phase could not be detected in the post-reaction X-ray diffractogram (Fig. 7d). Additionally, the C<sub>3</sub>H<sub>6</sub> combustion activity of 6Ag in the presence of water is lower than that shown by Ag/Al<sub>2</sub>O<sub>3</sub> catalysts with high silver loadings in other reports [12]. The fact that lower NO<sub>2</sub> yields are observed for the highest loaded sample also contrasts with the behaviour of similar systems in the literature [16]. On the basis of these results, it could be tentatively proposed, as an alternative possibility for the formation of metallic silver in 6Ag, that certain changes could be produced in the catalytic properties of amorphous silver oxide phases as a function of their relative particle size and/or of their degree of interaction with the underlying alumina. The presence of these amorphous phases could be related to the preparation method employed which includes a precipitation with an alkali. Under these conditions, some amount of surface Al can transfer to the aqueous phase affecting finally the larger Ag oxide particles, even if a definite silver aluminate phase were not formed. This would favour an amorphous character in the resulting ill-defined mixed oxide. In any case, it should be noted that no information is available on the changes undergone by the silver-containing phases over a large range of reaction temperatures, since only samples at the post-reaction temperature stage were studied. As proposed by

Bethke and Kung [12], it is possible that such metallic silver phases are stable only at certain reaction temperatures which cover the main reactivity range. The different behaviour of sample 6Ag with respect to other systems of similar characteristics [12,16] can also be related to the different conditions employed in the catalytic tests, considering that lower  $\text{N}_2\text{O}$  selectivities and  $\text{C}_3\text{H}_6$  oxidation activities are observed in the presence of water [12]. Lower propene oxidation activities have also been observed in the presence of water, as compared to dry reagent gases for other alumina supported systems [33]. It does not seem likely that results obtained for 6Ag could be the result of poisoning effects due to the presence of the  $\text{CO}_x$  or  $\text{NO}_x$  species observed in the spectrum of the initial calcined sample (Fig. 2). This statement is based on the fact that DRIFT spectra recorded at 723 K before recording the background spectrum prior to introduction of NO and  $\text{O}_2$  (Fig. 5a), show only a small band at  $1545\text{ cm}^{-1}$ , probably due to the presence of residual nitrate species. This was detected in the region corresponding to  $\text{CO}_x$  and  $\text{NO}_x$  (spectrum not shown), and showed considerably lower intensity than bands for similar species observed for sample 1.5Ag under reaction conditions at similar temperatures (Fig. 3).

To conclude, on the basis of comparisons between the different *in situ*-DRIFTS experiments, it is proposed that the main role of the most active silver-containing phases for  $\text{NO}_x$  reduction (as in 1.5Ag) lies in their capacity to activate  $\text{NO}_x$  species towards their reaction with the alumina support (via acidic hydroxyls), helping to maintain a relatively high concentration of adsorbed nitrate species at the catalyst surface. The small differences in intensities and nature of the hydroxyl species of initial 1.5Ag and 6Ag samples (Fig. 2) suggest in any case that deactivation of the silver–alumina interactions responsible for the catalytic activity cannot be attributed to blocking effects by silver of active sites on the support. It seems more likely that it is the different nature of the silver-containing phases in each case which determines the behaviour towards  $\text{NO}_x$  activation which leads as a consequence to the catalytic behaviour observed in each case. Deactivation of the 1.5Ag catalyst which is produced by brief pre-reduction in  $\text{C}_3\text{H}_6$  at 723 K (a treatment presumed to decrease the silver dispersion [16]), as inferred

from the experiments of Fig. 6, would support this argument.

### Acknowledgements

We thank L.N. Salamanca for performing the TEM experiments. A. Martínez-Arias wishes to thank the Comunidad Autónoma de Madrid for a post-doctoral grant and for financial help under the 'Ayudas para estancias breves en centros de investigación extranjeros' program. A. Iglesias-Juez thanks the Comunidad Autónoma de Madrid for a predoctoral grant. Support from CAYCIT (Project No. MAT 97-0696-C02-01) and CAM (Project No. 06M/084/96) is greatly appreciated.

### References

- [1] M. Iwamoto, S. Yokoo, K. Saaki, S. Kagawa, *J. Chem. Soc., Faraday Trans. 1* (77) (1981) 1629.
- [2] M. Iwamoto, H. Yahiro, K. Tanda, N. Mizuno, Y. Mine, S. Kagawa, *J. Phys. Chem.* 95 (1991) 3727.
- [3] J.O. Petunchi, W.K. Hall, *Appl. Catal. B* 3 (1994) 239.
- [4] V.I. Parvulescu, P. Grange, B. Delmon, *Catal. Today* 46 (1998) 233.
- [5] H.-W. Jen, *Catal. Today* 42 (1998) 37.
- [6] T. Miyadera, K. Yoshida, *Chem. Lett.* (1993) 1483.
- [7] R. Burch, P.J. Millington, A.P. Walker, *Appl. Catal. B* 4 (1994) 65.
- [8] R. Burch, T.C. Watling, *Appl. Catal. B* 11 (1997) 207.
- [9] T. Miyadera, *Appl. Catal. B* 2 (1993) 199.
- [10] S. Sumiya, M. Saito, H. He, Q.-C. Feng, N. Takezawa, K. Yoshida, *Catal. Lett.* 50 (1998) 87.
- [11] T. Miyadera, *Appl. Catal. B* 16 (1998) 155.
- [12] K.A. Bethke, H.H. Kung, *J. Catal.* 172 (1997) 93.
- [13] T. Nakatsuji, R. Yasukawa, K. Tabata, K. Ueda, M. Niwa, *Appl. Catal. B* 17 (1998) 333.
- [14] Z. Li, M. Flytzani-Stephanopoulos, *Appl. Catal. A* 165 (1997) 15.
- [15] M. Boutonnet, J. Kizling, P. Stenius, G. Maire, *Coll. Surf.* 5 (1982) 209.
- [16] F.C. Meunier, J.P. Breen, V. Zuzaniuk, M. Olsson, J.R.H. Ross, *J. Catal.* 187 (1999) 93.
- [17] H. Knözinger, P. Ratnasamy, *Catal. Rev. Sci. Eng.* 17 (1978) 31.
- [18] A.M. Turek, I.E. Wachs, E. DeCanio, *J. Phys. Chem.* 96 (1992) 5000.
- [19] A.A. Davydov, *Infrared Spectroscopy of Adsorbed Species on the Surface of Transition Metal Oxides*, Wiley, 1984.
- [20] T. Chafik, S. Kameoka, Y. Ukisu, T. Miyadera, *J. Mol. Catal.* A 136 (1998) 203.

- [21] S. Kameoka, T. Chafik, Y. Ukisu, T. Miyadera, *Catal. Lett.* 55 (1998) 211.
- [22] S. Sumiya, H. He, A. Abe, N. Takezawa, K. Yoshida, *J. Chem. Soc., Faraday Trans. 94* (1998) 2217.
- [23] M. Haneda, Y. Kintaichi, M. Inaba, H. Hamada, *Catal. Today* 42 (1998) 127.
- [24] K.-I. Shimizu, H. Kawabata, A. Satsuma, T. Hattori, *J. Phys. Chem. B* 103 (1999) 5240.
- [25] G.M. Underwood, T.M. Miller, V.H. Grassian, *J. Phys. Chem. A* 103 (1999) 6184.
- [26] J.A. Anderson, C.H. Rochester, *J. Chem. Soc., Faraday Trans. 1* (85) (1989) 1117.
- [27] T. Gerlach, F.-W. Schütze, M. Baerns, *J. Catal.* 185 (1999) 131.
- [28] K. Hadjiivanov, J. Saussey, J.L. Freysz, J.C. Lavalley, *Catal. Lett.* 52 (1998) 103.
- [29] T. Gerlach, U. Ilgen, M. Bartoszek, M. Baerns, *Appl. Catal. B* 22 (1999) 269.
- [30] A.D. Cowan, N.W. Cant, B.S. Haynes, P.F. Nelson, *J. Catal.* 176 (1998) 329.
- [31] S. Kameoka, T. Chafik, Y. Ukisu, T. Miyadera, *Catal. Lett.* 51 (1998) 11.
- [32] E. Seker, J. Cavataio, E. Gulari, P. Lorphongpaiboon, S. Osuwan, *Appl. Catal. A* 183 (1999) 121.
- [33] M. Haneda, Y. Kintaichi, H. Hamada, *Catal. Lett.* 55 (1998) 47.
- [34] T.H. Ballinger, J.T. Yates Jr., *Langmuir* 7 (1991) 3041.